

Non-stationary Physiological Noise in the Cardiovascular System during Sympatho-vagal Changes

Andrea Scarciglia,¹ Vincenzo Catrambone,¹ Claudio Bonanno,² and Gaetano Valenza¹

¹*Neurocardiovascular Intelligence Lab, Bioengineering and Robotics Research Center E.Piaggio & Department of Information Engineering, School of Engineering, University of Pisa, Italy;*

²*Department of Mathematics, University of Pisa, Italy;*

(*Electronic mail: andrea.scarciglia@phd.unipi.it)

This study introduces a novel estimation methodology for identifying non-stationary physiological noise, specifically applied to complex biomedical signals such as heart rate variability (HRV) series. By treating physiological noise as a dynamical recursive realization of independent and identically distributed (IID) Gaussian random variables, we employ an information-theoretic quantifier, the Approximate Entropy, to estimate noise power through a sliding window process. Our method effectively identifies noise levels in synthetic time series with varying dynamical noise powers, demonstrating accuracy even with relatively short window lengths. We further exploit this approach on real cardiovascular variability recordings during different postural changes, namely stand-up, slow tilt, and fast tilt. The results reveal significant time-resolved variations in physiological noise, functionally linked with changes in autonomic regulation due to postural shifts. Specifically, in the absolute sense, physiological noise in the cardiovascular system tends to increase in the first 60s of upright position with respect to a supine resting state, directly following sympathetic dynamics and inversely following vagal dynamics. Then, over 60s physiological noise tends to decrease with respect to the resting state, almost monotonically. Moreover, results corroborates earlier findings where elevated stochasticity in HRV series biases complexity assessment through entropy analysis. Our work highlights the method's robustness and potential to improve the understanding of physiological noise dynamics, with implications for more accurate cardiovascular signal analysis and potential clinical applications.

We provide key insights into the role of stochasticity in non-stationary cardiac autonomic regulation during sympathovagal changes. By leveraging a sample-by-sample nonlinear Approximate Entropy profile, our approach accurately captures time-resolved variations in physiological noise, even with short window length. The findings indicate that reduced vagal activity and increased sympathetic activity are associated with higher stochasticity in the cardiovascular system. This methodology enhances the understanding of physiological noise dynamics and improves the accuracy and reliability of cardiac complexity assessments, with promising implications for clinical monitoring and decision support systems.

I. INTRODUCTION

Time series stationarity refers to the constancy of the system's statistical properties over time¹. The concept of stationarity plays a fundamental role in time series analysis. Stationarity is often assumed in many analytical tools derived from both linear and nonlinear signal processing frameworks, including, autoregressive models, embedding dimensions, spectral analysis, entropies, information theory frameworks, and models or predictions of data series using local linear models, radial basis functions, neural networks, and nonlinear stochastic processes^{2,3}.

Physiological signals are susceptible to various external factors, e.g. measurement artifacts, and intrinsic dynamic behaviors, potentially resulting in non-stationarity or long-term

correlations. Non-stationarity makes frequency domain analysis simply unreliable and may generate erroneous chaotic-like behavior based on some properties of their nonlinear features, such as correlation dimension and Kolmogorov entropy⁴.

The cardiovascular system is primarily explored through the analysis of heart rate variability (HRV) time series, which represent the time intervals between consecutive R peaks in the electrocardiogram of humans. HRV is regulated by the concurrent action of the sympathetic and parasympathetic branches of the autonomic nervous system (ANS), as well as by baroreflex and respiration activity⁵. Particularly, the cardiovascular system is well-recognized for its nonlinear and non-stationary nature of its dynamics⁶, given by complex self-regulating processes which are characterized by long-range dependence⁶ - reflected in the $1/f$ spectrum scaling law -, and that are associated with multifractality, requiring a large number of exponents to characterize their scaling properties⁷. The nonlinear interplay in ANS dynamics^{8,9} makes HRV series exhibit complex patterns^{10,11} marked by unpredictability, bifurcation, intermittent and scale-invariant behavior⁷. In particular, the multifractal nature of physiological processes - also evident in cardiovascular activity - has played a key role in several domains including causal and network modeling¹²⁻¹⁶, as well as characterization of specific pathological conditions¹⁷⁻¹⁹.

To this end, the time and frequency domain analyses of long-term (e.g. 24h) HRV series should be performed in shorter time segments, typically around 5 minutes, and then outcomes should be aggregated²⁰.

Another critical component of cardiovascular dynamics is the presence of intrinsic, recursive stochastic components,

also known as physiological noise²¹. For many years, the challenge of discerning deterministic and stochastic components in heartbeat dynamics has been investigated. However, a universally accepted characterization is still lacking. The debate continues on whether cardiovascular variability series are chaotic (and thus deterministic) or purely stochastic. This uncertainty arises from the lack of a definitive model for RR intervals, despite extensive research. The complexity of HRV series may be discussed without clearly labeling it as chaotic or stochastic.

This ambiguity is reflected in past studies, as noted in a seminal paper²². To illustrate, some works, using scale-dependent Lyapunov exponents, highlight varying shades of stochasticity across patho-physiological states²³. Others, employing the Largest Lyapunov Exponent, suggest a chaotic nature rooted in autonomic control loops²⁴, as also observed in atrial fibrillation through permutation entropy and missing ordinal patterns²⁵. This chaotic behavior may be influenced by stochastic fluctuations in acetylcholine²⁶, while other studies point to coupled deterministic oscillators and respiratory-driven stochastic components^{27,28}. In our study, rather than aligning strictly with one perspective, we adopt a hybrid framework: cardiovascular dynamics is modeled as the output of a nonlinear deterministic system⁹ perturbed by dynamical noise, which irreversibly modifies the behavior of the system, leading to an overall alteration in its dynamics. In this context the heartbeat series reveal inherent physiological noise due to the continuous dynamic interaction of the cardiovascular system with various other physiological subsystems (such as endocrine, neural, and respiratory systems)²⁹, as well as numerous self-regulating, adaptive biochemical processes¹¹. Essentially, such an informative noise not only has the potential to substantially impact the functioning of physiological systems but is also an integral aspect of their dynamics. Physiological systems are recognized as complex dynamical systems, particularly nonlinear systems influenced by stochastic inputs (i.e., noise), which can lead to the emergence of chaotic regimes^{30,31}. Recently, this physiological noise has been quantified in physiological time series^{21,32}, especially in HRV time series, characterizing different pathophysiological states within a framework that does not necessitate knowledge of the underlying deterministic dynamics, often unknown in physiological time series or real-world data in general.

To our knowledge, no previous attempts have been made to identify physiological noise non-stationarity as an inherent characteristic of the cardiovascular system. In this study, we build on the approach outlined in³³ to develop an effective methodology that captures dynamical changes in physiological noise over time. First, the proposed sample-wise physiological noise estimation methodology is validated using synthetic data perturbed by dynamical non-stationary noise. Then, the method is applied to real HRV time series to assess noise variability during postural changes, which are known to induce strong sympathovagal changes and, consequently, non-stationarity in the HRV series^{34–36}. Specifically, standing causes a decrease in blood pressure that leads to increased heart rate, cardiac contractility, and peripheral vascular resistance³⁷. Moreover, the transition from rest to an

upright position is associated with a decrease in heartbeat complexity^{38–40} as well as a decrease in HF power³⁵. Therefore, while the resting supine position is associated with a dominance of cardiac vagal activity⁴¹, the upright position is associated with a dominance of sympathetic activity and vagal withdrawal, the dynamics of which depend on the kind of transition³⁵. The tilt-table test is thus commonly employed as a gold-standard protocol to induce sympathovagal changes and diagnose conditions such as vasovagal syncope (fainting) and orthostatic hypotension.

II. NON-STATIONARY PHYSIOLOGICAL NOISE

The sampled physiological signal $x_n(\varepsilon)$ is regarded as an output of a dynamical system (X, μ, F) , where μ is the invariant probability measure of the phase space X on which the differentiable map F defines the deterministic dynamical model, and $\{\varepsilon_n\}_n$ are realizations of physiological noise modeled as independent and identically distributed (IID) Gaussian random variables $\mathcal{N}(0, \sigma)$. In a general case, physiological noise perturbs the system dynamics according to:

$$x_n = F(x_{n-1}, \dots, x_1) + \varepsilon_n \quad (1)$$

where x_n are the points belonging to the space X . It is assumed that the time series non-stationarity is due to the related stochastic components, i.e. the dynamical noise power.

Hereinafter, we focus on heartbeat dynamics series whose samples, occurring in the continuous time t , are intrinsically discrete and are associated with the R-wave events $\{u_j\}_{j=1}^N$ detected from the ECG. To this extent, $RR_j = u_j - u_{j-1} > 0$ denotes the j^{th} R–R interval.

Formally, for $t \in (0, T]$, the observation interval, and $0 \leq u_1 < \dots < u_j < u_{j+1} < \dots \leq T$ the times of the heartbeat events, let us define

$$N(t) = \max\{j : u_j \leq t\}$$

as the sample path of the associated counting process. Its differential, $dN(t)$, denotes a continuous-time indicator function, where $dN(t) = 1$ when there is an event, and $dN(t) = 0$ otherwise. The left continuous sample path is defined as

$$\tilde{N}(t) = N(t^-) = \lim_{\tau \rightarrow t^-} N(\tau) = \max\{j : u_j < t\}$$

such that the cardiovascular system dynamics may be described as:

$$RR_{\tilde{N}(t)} = F(RR_{\tilde{N}(t)-1}, \dots, RR_{\tilde{N}(t)=0}) + \varepsilon_{\tilde{N}(t)} \quad (2)$$

with $\tilde{N}(t)$ is the index of the previous R-wave event before time t and F is an unknown, linear or nonlinear function.

Within this framework, it is possible to estimate the physiological noise standard deviation σ without knowing the map F , by using the information-theoretic quantifier Approximate Entropy (ApEn)⁴², and applying the closed formula³³:

$$\log(\sigma|W) \approx \text{ApEn}(\{RR_{\tilde{N}(t)}(\varepsilon)\}_{t=1}^{T'}, m, r) + \log(r/\sqrt{\pi}) \quad (3)$$

considering observations of RR intervals within a time window W defined in $(0, T']$, for any embedding dimension m , when the tolerance or radius r is smaller than the noise standard deviation σ . More details on the noise estimation procedure and its theoretical foundation can be found in^{32,33}. The procedure described above requires the stationarity of the physiological noise process within the time interval $t \in (0, T']$, implying that the physiological noise power does not change over the entire series.

Next, we proceed with a non-stationary, sample-wise estimation of the physiological noise process.

Let us consider s subsets of the sampled series $RR_{\tilde{N}(t)}(\varepsilon(t))$. The physiological noise process is stationary within each subset, such that there exists a finite sequence $\{\varepsilon_{\tilde{N}(t)}\}_{t=t_j}^{T'} \sim \mathcal{N}(0, \sigma_{\tilde{N}(t)})$. Therefore, we can evaluate the non-stationary physiological noise standard deviation as follows:

$$\Psi_{RR}(t', \mathcal{H}_{t'}, \varepsilon(t')) \approx$$

$$\exp(\text{ApEn}(\{RR_{\tilde{N}(t)}(\varepsilon(t))\}_{t=0}^T W(t-t'), m, r(t'))r(t')/\sqrt{\pi} \quad (4)$$

where $\mathcal{H}_{t'} = (u_{\tilde{N}(t')}, RR_{\tilde{N}(t')}, RR_{\tilde{N}(t'-1)}, \dots, RR_{\tilde{N}(t'-T'+1)})$.

Practically, one does not know *a priori* the temporal intervals where noise achieves stationarity. Thus, we select a rectangular time window W comprising w samples and, for each subseries $\varepsilon_{n=i}^{i+w}$, we perform a sample-wise estimation of $\Psi_{RR}(i, \mathcal{H}_{t'}, \varepsilon(t'))$.

III. EXPERIMENTAL DATA AND SETUP

We tested the proposed sample-wise estimation methodology in detecting variations in noise non-stationarity in synthetic time series corrupted with different levels of dynamical noise. The noise estimation is performed sample-wise on overlapping windows of a fixed length that slide along the entire time series.

After verifying the reliability of the method, we applied the noise estimation to heartbeat time series gathered from a dataset comprising HRV recordings of subjects undergoing different postural changes (stand-up, slow, and fast tilt). This was performed to determine if the physiological noise power varies during these different tasks.

Analytical Data

The proposed approach has been tested on synthetic series gathered from:

Discrete-time Logistic Maps: which are maps of the following form

$$x_{n+1} = \lambda x_n(1 - x_n) \quad (5)$$

where λ is a real-valued parameter in the interval $[0, 4]$ and at step n , all the x_n belong to the interval $[0, 1]$. The discrete-time logistic map is a simple mathematical model that describes the dynamics of a population over time. It is a nonlinear difference equation that can exhibit a wide range of behaviors, from stable equilibrium points to chaotic oscillations, accordingly to the parameter λ . Numerical simulations in this work are performed with $\lambda = 3.5$, in periodic regime and with $\lambda = 4$, namely in chaotic regime (Kolmogorov-Sinai entropy > 0). Dynamical noise effects are imposed by adding a noise sample at each step in 5.

For each value of the parameter λ above, we generated 50 time series with non-stationary Gaussian dynamical noise.

Autoregressive models of order p (AR(p)): the realization of an autoregressive model of order p , denoted as AR(p), can be expressed as follows:

$$y_n + \sum_{i=1}^p a_i y_{n-i} = \varepsilon_n,$$

where y_n is the n -th observation in the time series, a_i are the p time-invariant coefficients, and ε_n is the innovation process, namely a realization of an IID Gaussian stochastic variable. We performed our analyses selecting an AR model with order $p = 7$ (AR(7)) with the following parameter values: $a_1 = -1.2710$, $a_2 = 0.4222$, $a_3 = -0.0528$, $a_4 = -0.0544$, $a_5 = 0.0879$, $a_6 = 0.0446$, $a_7 = -0.1760$. These values were obtained by fitting the Yule-Walker equations to a random exemplary Heart Rate Variability series of a healthy subject from the database <https://physionet.org/content/nsrdb/1.0.0/>, considering only the first 500 points to avoid non-stationarity. The order $p = 7$ has been selected because in computational physiology cardiovascular dynamics has been modeled through an AR(7) model⁴³.

We considered 50 series for the AR(7) model with non-stationary Gaussian noise.

Synthetic HRV series: the non-stationary noise detection has been applied also on noisy HRV series generated by the well-known *integral pulse frequency modulation* (IPFM)⁴⁴ model. The latter employs a network of interconnected oscillators, with each oscillator representing a distinct aspect of the baroreflex and autonomic nervous system.

The sympathetic oscillator is characterized by a sinusoidal waveform with a frequency of ω_s and represents the combined low-frequency (LF) power of the HRV spectrum, incorporating vasomotor activity. Conversely, the parasympathetic respiratory oscillator is modeled as a sinusoidal waveform with a frequency of ω_p and aims to capture short-term activity affecting the sinus node through the parasympathetic nervous system.

The autonomic activity, i.e. the combination of the parasympathetic and sympathetic activities, is represented by the quantity

$$m(t) = C_s s(t) + C_p p(t)$$

where $s(t)$ and $p(t)$ denote the sinusoidal waveform of the sympathetic and parasympathetic activity, respectively, and

where the coupling constants C_s and C_p indicate the degree to which the respective oscillator influences the sinus node oscillator, with s representing sympathetic and p representing parasympathetic modulation.

The heartbeat series, instead, is generated by integrating an input signal until it reaches a preset threshold of unity. At this point, a pulse is produced and the integrator is reset to zero. Mathematically, the time t_k of the k^{th} R wave is given by

$$1 = \int_{t_k}^{t_{k+1}} [HR + m(t)] dt \quad (6)$$

where $m(t)$ is the input signal of the autonomic activity and HR represents mean heart rate. Further details on the model can be found in⁴⁴.

In this work, $\omega_s = 0.1Hz$, $\omega_p = 0.25Hz$, $C_s = C_p = 0.15$, $HR = 1.1$ with a sampling rate of $250Hz$ for the generation of the HRV signals.

50 HRV noisy series of 20000 samples have been generated. We simulated the dynamical noise action by adding a sample of the noise realization process at the integrand function of each integration step (6).

To reproduce the effects of non-stationary noise, for all the previous models, we concatenated 4 realizations of the same models consisting of 5000 samples, where the i^{th} series is corrupted by dynamical noise according to eq. (2) as a realization of IID random variables following the distribution $\mathcal{N}(0, \sigma_i(W))$, where: $\sigma_1 = 0.05, \sigma_2 = 0.1, \sigma_3 = 0.15, \sigma_4 = 0.2$ for the logistic maps; $\sigma_1 = 0.5, \sigma_2 = 1, \sigma_3 = 1.5, \sigma_4 = 2$ for the AR(7) model; $\sigma_1 = 0.8, \sigma_2 = 1.2, \sigma_3 = 1.6, \sigma_4 = 2$ for the IPMF HRV model.

To ensure that all samples in the time series remain within the range of $[0, 1]$ without drifting, we apply a modulo 1 reduction at each step of (5) for the logistic map.

Eventually, each synthetic series has 20000 samples formed by 4 different realizations (5000 points each) where an always different noise realization has been superimposed.

We have applied the sample-wise non-stationary noise detection with different overlapping time window comprising $w = 100, 150$ and 200 , with an embedding dimension $m = 2$ and letting the radius r spanning the time series amplitude within the window with a resolution step $\Delta r = 0.001 \times \{\text{time series range}\}$ for all the series.

The sensitivity of the proposed method has been tested by generating 30 synthetic time series, each containing 10000 samples. Each series consisted of 20 segments of 500 points derived from a nonlinear Logistic map with a parameter of $\lambda = 3.5$, without loss of generality. These segments featured increasing dynamical noise levels, ranging from 1% to 20% with a 1% step with respect to the time series amplitude. Time-variant noise estimation techniques are applied using sliding windows of 100, 150 and 200 samples.

Moreover, to validate the proposed method's independence from the influence of underlying dynamical systems' behaviors, in contrast to conventional HRV quantifiers, we generated 30 time series by concatenating 3000 points from a lo-

gistic map with parameter $\lambda = 3.5$ and 3000 points from a logistic map with parameter $\lambda = 4$, both perturbed with zero-mean Gaussian noise with a standard deviation of 0.05. The two maps exhibit different dynamics: the first is periodic, while the second is chaotic. On this maps we have computed sample-wise STD and noise estimation within a sliding window of 1000 samples.

Real HRV series during Postural Changes

We tested the sample-wise noise estimation power on real HRV series gathered from the *Physiologic response to changes in posture* dataset³⁴, publicly available⁴⁵. The dataset was generated to measure the extent of similarity in hemodynamic responses observed during stand-up, rapid, and slow head-up tilt (HUT). This initiative stems from limited understanding of the mechanisms involved in orthostatic intolerance, which refers to the failure of the hemodynamic system and reflex mechanisms to maintain blood pressure homeostasis. The dataset comprises data collected from ten healthy volunteers (five males and five females, with an average age of 28.7 ± 1.2 years). The participants gave informed written consent for the procedure, and the signals were acquired using a standard clinical ECG device. The experimental protocol consisted of a 5-minute resting state, followed by a series of postural changes, from the horizontal to the vertical position and returned to the horizontal position either through a "slow" tilt (50 s from 0 to 70°), or "fast" (i.e., 2 s from 0 to 70°), each lasting for 3 minutes. Stand-up sessions were also included. Approval for the experimental procedure was obtained from the local ethical committee, and further information can be found in³⁴. The ECG data underwent analysis using the Pan-Tompkins algorithm⁴⁶ to detect the R-peaks and generate the HRV series. Additionally, the series underwent preprocessing using a point-process-based model⁴⁷ to remove ectopic and erroneous heartbeats. Further information can be found in³⁴.

We performed sample-wise non-stationary noise detection with various overlapping time windows, each consisting of 150 data points. We set the embedding dimension to $m = 2$ and adjusted the radius r to cover the amplitude of the time series within the window, using a resolution step of $\Delta r = 0.001 \times \text{time series range}$ for all the recordings.

The non-stationarity of the real HRV series and of the related estimated noise time series, restricted to 60s before up to 180s after every postural change, are assessed through the Kwiatkowski-Phillips-Schmidt-Shin (KPSS) test with null hypothesis of stationarity (against the alternative hypothesis of non-stationarity) and the complementary Phillips-Perron (PP) test (null hypothesis of non-stationarity and alternative hypothesis of stationarity), with a significance threshold of 0.05.

Statistical differences between superimposed noise levels, as well as supine vs. upright positions were assessed through the non-parametric Wilcoxon test for paired samples with the null hypothesis of equal noise levels median before and after postural changes.

This study received approval from the University of Pisa's Committee of Bioethics under review number 19/2021 and adhered to the principles outlined in the Declaration of Helsinki.

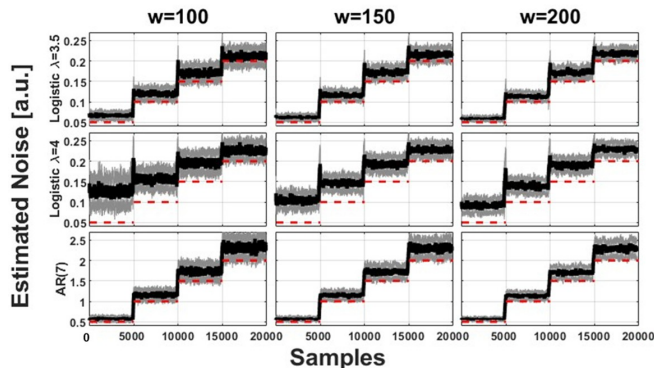


FIG. 1. Sample-wise noise estimation for synthetic maps expressed as median (black line) \pm median absolute deviation (shaded area) among 50 realizations of the five synthetic data models individuated by the rows. Red lines indicate true reference values. In each panel, the local noise std (y-axis) is illustrated along with the time series length (x-axis). Estimations have been performed with embedding dimension $m = 2$, $\Delta r = 0.001 \times \{\text{time series range}\}$ and within an overlapping time window starting from the sample and comprising w points ahead. Window lengths are indicated by the figure columns.

IV. RESULTS

Synthetic data

Analytical maps: Figure 1 presents the results of sample-wise noise estimation for synthetic data gathered from the logistic maps and the AR(7) model. Each row refers a distinct model, while each column indicates the length of the sliding window w used for the local noise estimation.

In each panel, the sample-wise noise estimation (y-axis) is depicted in terms of the median and median absolute deviation (MAD), shown with thick lines and shaded areas, respectively, across 50 realizations within a time window starting from the current point (x-axis) of the time series.

The proposed method effectively distinguishes different levels of non-stationary noise in time series, both qualitatively and quantitatively, even when the sliding window contains a small number of samples. The red horizontal dashed lines correspond to the four variations of injected noise, as discussed in the previous section. Generally, increasing the sliding window size improves noise detection accuracy by reducing dispersion around the median value. The method also identifies transition zones where statistical noise power changes, which are aligned with the steps of the horizontal red dashed lines.

Specifically, higher levels of encountered non-stationary noise exhibit greater variability, indicating the need for a larger number of samples to accurately identify the underlying noisy dynamics. For the logistic map in the periodic regime ($\lambda = 3.5$) and the AR(7) model, the estimated noise values

closely match the actual superimposed ones. In contrast, for the logistic map in the chaotic regime ($\lambda = 4$) there is a slight overestimation that tends to decrease with larger sliding windows. Additionally, noise estimates are smooth for all models except for the chaotic logistic map, which exhibits spikes that are mitigated by using longer time windows.

For the IPFM HRV model, the results in Figure 2 show, across different rows, the mean, standard deviation (STD), root mean square of successive differences (RMSSD), as well as the low-frequency (LF) and high-frequency (HF) powers, and the proposed physiological noise estimation ψ_{RR} . It is evident that while the window length does not significantly affect the estimates, all metrics increase as physiological noise increases, except for the mean values, which remain approximately constant in terms of central tendency. Importantly,

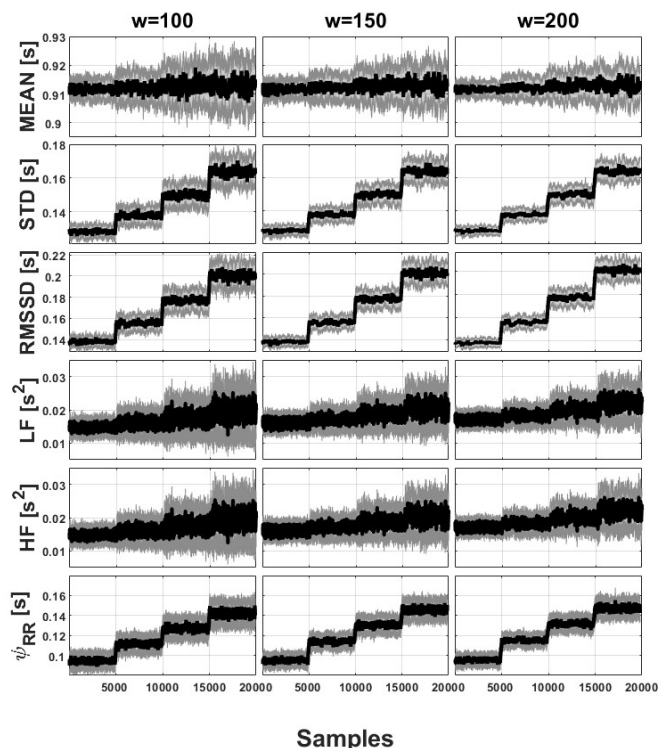


FIG. 2. **Sample-wise statistics and noise estimation for the IPFM model.** Sample-wise estimates of mean, STD, RMSSD, LF power, HF power, and estimated physiological noise are reported on the rows for the IPFM synthetic model, computed across 50 realizations. Each panel illustrates the evolution of these statistics (y-axis) over time (x-axis) within overlapping windows of varying lengths (columns). For LF and HF power estimation, time series were interpolated to 4 Hz. Noise estimation was performed using an embedding dimension (m) of 2 and a radius (r) that spans the time series amplitude within the window, with a resolution step of $\Delta r = 0.001 \times \{\text{time series range}\}$. The shaded area in each panel represents the median absolute deviation (MAD) around the median value (black line).

these results demonstrate that changes in time and frequency domain parameters, which are usually linked to sympathetic and vagal activity changes, may actually be generated by

underlying stochastic changes rather than cardiac neural activity. Indeed, such HRV standard estimates do not discern between deterministic and stochastic dynamics.

To further demonstrate this evidence, regarding the possible quantifiers' dependence on the underlying dynamics, results in estimating STD and time-varying noise within overlapping 1000-sample windows of Figure 3 show that STD significantly changes between maps, whereas our proposed method does not exhibit such variability. This aligns with our theoretical claim that our method detects noise as an intrinsic component of the system, independent of the underlying dynamics.

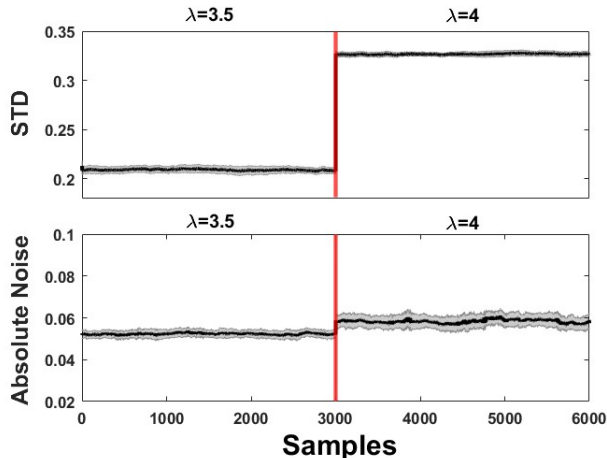


FIG. 3. Sample-wise STD and noise estimation for exemplary series with two different dynamics. This figure depicts sample-wise estimates of standard deviation (STD) (top row) and encountered noise (bottom row) for 30 realizations. Each realization consists of 6000 samples, combining 3000 samples from a periodic logistic map ($\lambda = 3.5$) with 3000 samples from a chaotic logistic map ($\lambda = 4$). Both segments are corrupted by the same level of dynamic noise, generated from a normal distribution with mean 0 and standard deviation 0.05. The vertical red line marks the transition between the periodic and chaotic segments. Sample-wise estimates were calculated using overlapping windows of 1000 samples. The black line represents the median value, and the shaded area depicts the median absolute deviation (MAD) across the 30 realizations.

Sensitivity: The results, shown in Figure 4, illustrate the median absolute noise sample-wise estimation (black line) across the 30 time series, with the dispersion around the median (shaded areas), using windows of 100, 150 and 200 samples (from left to right). The linear fit (red line) of the median estimated noise is also represented. The figure highlights distinct steps corresponding to the varying noise levels. These transitions are often preceded by spikes, which are artifacts coinciding with abrupt changes in noise magnitude. Longer window sizes tend to improve the accuracy of the estimated noise levels and reduce the prominence of these spikes, resulting in smoother intervals corresponding to the estimated noise levels. The slope of the red line, fitted to the median noise estimates, indicates the method's sensitivity. Since the slopes of the fitted lines were 0.0228%, 0.0166%, and 0.013%

from the smallest to the largest window, we can conclude that the length of the time window does not significantly affect the time-varying estimation.

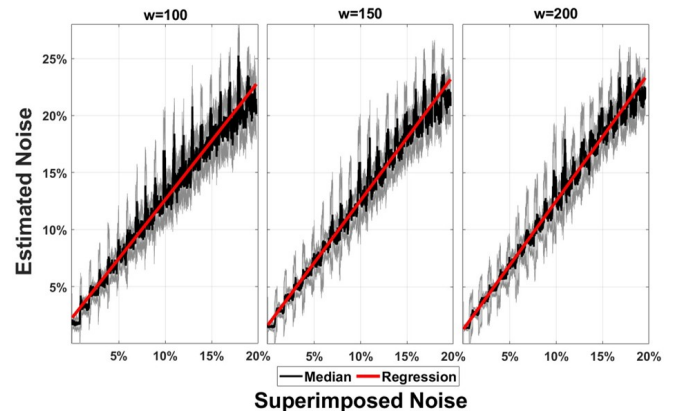


FIG. 4. Sensitivity analysis on the Logistic map with ($\lambda = 3.5$). The figure displays the median (black line) of the time-varying noise estimated over 100-, 150- and 200-sample windows (from left to right, respectively) across 30 realizations of the logistic map. The shaded area represents the median absolute deviation, and the red line is the fitted median. The x-axis shows the introduced dynamic noise levels, while the y-axis displays the estimated noise levels as a percentage of the series amplitude. The variation of injected noise is of 1% between consecutive levels.

Real Data

Non-stationarity: Regarding real data, non-stationarity of all the HRV and estimated noise series has been assessed by the rejection of null hypothesis for the KPSS test together with the non-rejection of the null hypothesis of the PP test. A visual representation of the non-stationarity in the estimated noise time series is shown in Fig. 5, where spectrograms of the estimated absolute noise time series during postural changes are reported.

Physiological Noise Estimation: Numerical results of the real data analysis are reported in Fig. 6 as the sample-wise median \pm MAD among subjects, normalized according to the number of trials, of the encountered sample-wise noise estimation across the several trials of postural changes. The figure illustrates the physiological noise trends during the slow, fast tilt, and stand-up transitions from the supine resting state to the vertical position. The middle panel represents the standardized noise measure with respect to the standard deviation of the signal enclosed in the window. At the bottom panel, the average RR interval \pm the RR interval standard deviation across all the trials of postural changes are illustrated. In all the figures, noise estimates and HRV series have been interpolated over the recording time, with a frequency of 2Hz, to allow comparisons among all the rest and tilt phases of the HRV recording. Starting from the postural change onset, the estimated physiological noise begins to reflect the effects of the postural changes. Descriptive and inferential statistics are

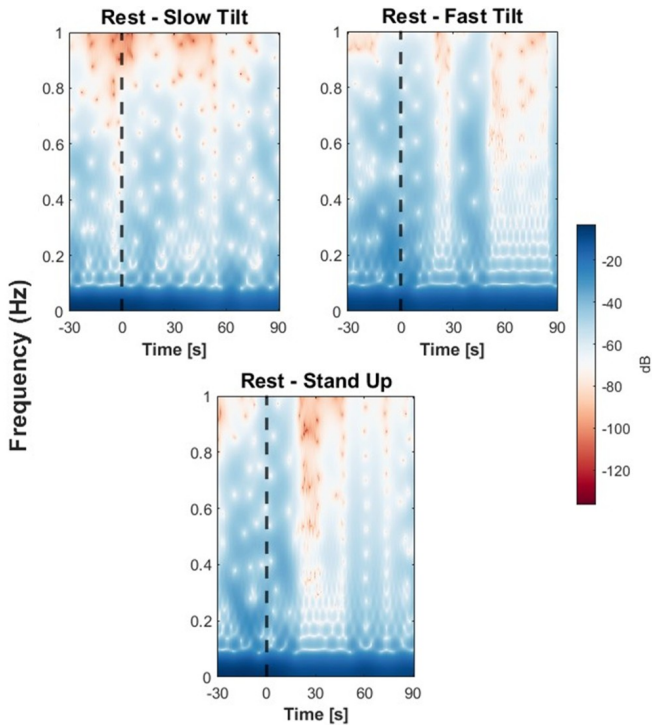


FIG. 5. **Exemplary Spectrograms of the estimated absolute noise time series.** The figure represents the spectrograms of the estimated noise time series from the HRV recording of subject 12726 of the dataset of postural changes. Each panel corresponds to the first different transition from rest to postural tasks. The dashed black line indicates the beginning of the task. Blue color denotes higher magnitude. Spectrograms are generated from the interpolation of absolute noise time series at 2Hz, from 30s before up to 90s after the postural change from rest condition. The spectrograms are computed with the short-time Fourier transform, by using Hanning window with amplitude of 20s and with the temporal shift of 0.5s - 97.5% of overlap between consecutive windows.

reported in Table I for all experimental sessions. It is evident that the sliding windows capture transitions from rest to postural changes as expressed by an increase in absolute physiological noise levels, especially in case of fast and stand-up tilts. After about 60s from the postural change onset, the absolute physiological noise levels decrease significantly (Wilcoxon test p -value less than 10^{-6}). It is possible to notice that all HRV features but the LF power are significantly affected by the postural changes.

V. DISCUSSIONS AND CONCLUSIONS

In this study, we present a method for detecting physiological noise non-stationarity in complex physiological time series. The proposed framework treats physiological noise as a recursive realization of IID random variables, typically Gaussian $\mathcal{N}(0, \sigma)$. Despite the potential for alternative noise distributions, the inherent recurrence of physiological noise causes it to accumulate within the system through repeated iterations. Thus, positing that the physiological noise is

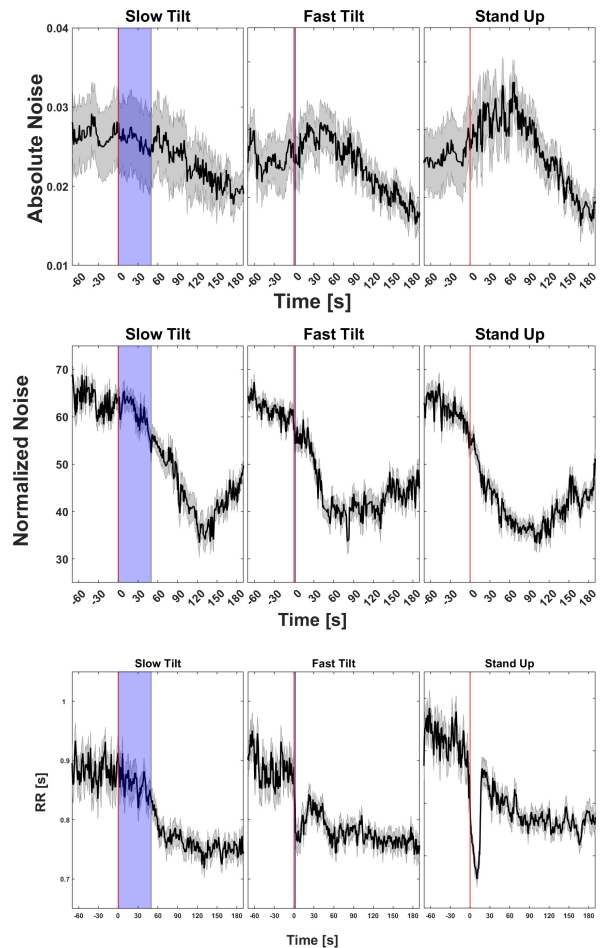


FIG. 6. **Physiological Noise in the TILT dataset.** The figure shows the group-wise median (black lines) and median absolute deviation (shaded areas) values of absolute noise (upper panels) and normalized noise (middle panels), as well as RR intervals before and after the onset (indicated by the vertical red line) of postural change tasks (slow tilt, fast tilt, and stand-up). The normalized physiological noise is calculated relative to the series' standard deviation. Blue shaded areas indicate the time window during which the postural changes are performed.

composed of independent and identically distributed random variables, where the statistical distribution remains constant across iterations, the central limit theorem predicts that the aggregated sum will tend towards a Gaussian distribution. This detection is achieved through a window-sliding process, which returns a sample-wise physiological noise power estimation $\Psi_{RR}(t', \mathcal{H}_t, \varepsilon(t'))$ and its variability throughout the entire series. We tested the method on four different classes of synthetic time series and applied it to real cardiovascular data gathered from a publicly available postural changes dataset to detect possible variations during significant sympathetic changes, recognizing the fundamental, intrinsic role of stochastic dynamics in the cardiovascular system.

For synthetic data, the method effectively differentiated different levels of superimposed dynamical noise using a rel-

TABLE I. **P-values of resting vs. postural changes.** The table reports the statistics (median and median absolute deviation) computed over a 15-second window before the task and a similar window at the end of the task, for the encountered noise levels sample-wise STD, mean, RMSSD, LF and HF power. The significance of the differences in noise levels due to postural changes is confirmed by the p-values from the Wilcoxon tests, which test the null hypothesis of equal medians before and after the postural alterations.

		Rest	Slow Tilt	Rest	Fast Tilt	Rest	Stand Up
Absolute Noise [s]	Median	0.0264	0.0185	0.0264	0.0201	0.0273	0.0197
	MAD	0.01977	0.0084	0.0179	0.01	0.0222	0.0106
	p-value	< 10 ⁻¹⁰		< 10 ⁻¹⁰		< 10 ⁻¹⁰	
Normalized Noise	Median	62.1906	50.0448	60.6042	44.34795	59.5101	43.343
	MAD	8.7	8.23	7.34	9.84	9.24	8.56
	p-value	< 10 ⁻¹⁰		< 10 ⁻¹⁰		< 10 ⁻¹⁰	
Mean [s]	Median	0.8691	0.7529	0.905	0.7792	0.9362	0.7874
	MAD	0.13	0.0665	0.1053	0.0594	0.1106	0.068
	p-value	< 10 ⁻¹⁰		< 10 ⁻¹⁰		< 10 ⁻¹⁰	
SDNN [s]	Median	0.0445	0.0375	0.044	0.0482	0.0451	0.0509
	MAD	0.0258	0.0146	0.0274	0.0173	0.0414	0.0174
	p-value	< 10 ⁻¹⁰		0.1305		< 10 ⁻¹⁰	
RMSSD [s]	Median	0.0318	0.0193	0.0323	0.0205	0.0351	0.0213
	MAD	0.0309	0.0104	0.0236	0.013	0.0361	0.0131
	p-value	< 10 ⁻¹⁰		< 10 ⁻¹⁰		< 10 ⁻¹⁰	
LF [s²]	Median	0.001	0.0009	0.001	0.0011	0.0012	0.0016
	MAD	0.0023	0.001	0.0017	0.0018	0.0032	0.0025
	p-value	0.3281		0.1935		0.3885	
HF [s²]	Median	0.0005	0.0002	0.0006	0.0002	0.0006	0.0003
	MAD	0.0029	0.0007	0.0018	0.0008	0.0044	0.0013
	p-value	< 10 ⁻¹⁰		< 10 ⁻¹⁰		< 10 ⁻¹⁰	

actively short window length of only 100 samples, as confirmed by sensitivity analysis which retraces the imposed variation and validates the noise changes found by our time-variant method. This is notable because the noise estimation algorithm³³ theoretically requires a large number of samples to perform accurately. The accuracy of sample-wise noise estimation along the series improves with larger time windows, as evidenced by decreased dispersion around the median value, resulting from a more precise characterization of the approximate entropy quantifier. Moreover, for periodic dynamics and autoregressive models, the sample-wise noise estimation appears extremely accurate. In contrast, for chaotic dynamics, we observe a slight overestimation of noise levels due to the need for more samples to properly distinguish the dynamics from the noise presence. In smaller sample observations, the series might appear more random, obscuring the underlying dynamical pattern.

A separate discussion is necessary for IPFM HRV model, as its formulation inherently involves stochastic perturbations interacting with a dynamical component or multiple integration processes. Indeed, the noise observed in IPFM HRV models tends to be significantly underestimated. This discrepancy may be attributed to the unique nature of the IPFM model, which generates heartbeat series by integrating an input signal until it reaches a predetermined threshold parameter. When noise is introduced into the integration process, predicting how the noise samples interact becomes challenging. There's a possibility that they cancel each other out, given their mean is 0, as per the assumptions. Nonetheless, the pro-

posed method distinctly discern between different levels of dynamical noise in a time-resolved way. All classical time and frequency domain quantifiers exhibit a similar trend to our time-varying noise estimate, which is expected given the relationship between noise and signal variability. However, our method, which is less sensitive to underlying dynamics, reveals that changes in time and frequency domain parameters, commonly associated with sympathovagal and vagal activity, may be attributed to stochastic fluctuations rather than neural mechanisms. This has also been further demonstrated by the synthetic data analysis shown in Figure 3.

The proposed method finds a natural application on the HRV time series gathered from the postural changes dataset, since both the PP and KPSS tests confirmed the non-stationarity of the physiological time series undergoing the different tasks. Results showed that physiological noise in the cardiovascular system tends to increase from supine rest to upright standing. This increase is more pronounced during the first 60s of stand-up or fast tilt transitions from rest. Subsequent changes show a significant decrease in physiological noise levels with respect to the supine resting state. Normalized physiological noise dynamics significantly decreases after posture changes. Specifically, the proportion of heartbeat dynamics explained by noise is around 60-70% during rest and decreases to 30-40% in the upright position. Interestingly, the transition from rest to slow tilt is associated with a minimum physiological noise approximately 120 seconds after the tilt onset, while the minimum is reached around 60 seconds after the fast tilt and stand-up tasks. These findings demonstrate that physiological noise is not merely a constant in the dynamics, but rather an intrinsic and non-stationary component of the system — as confirmed by statistical tests and by the time-dependent frequency modulation in the spectrograms of the estimated noise time series — thus variable and informative of the system's state.

At a speculative level, these results suggest that the intrinsic stochasticity in cardiovascular dynamics is primarily driven by an increase in sympathetic activity coupled with a withdrawal of vagal activity, as absolute physiological noise trends mirror those of sympathetic activity³⁵. Conversely, normalized noise dynamics appear to follow vagal activity³⁵. Notably, the reduction in vagal and normalized noise due to postural changes is consistent with earlier research showing reduced cardiovascular complexity during posture changes³⁹. From a biochemical perspective, while its precise origin remains elusive, this non-stationary physiological noise likely arises from the complex interplay within the autonomic nervous system²⁴ - cardiovascular dynamics exhibit inherent non-linearity and are influenced by physiological randomness. Neurotransmitters like norepinephrine, released by the sympathetic nervous system, and acetylcholine, released by the parasympathetic system, along with other mediators, contribute to this stochasticity^{11,48,49}. Our findings suggest that previous entropy-based complexity assessments of HRV series may be influenced by natural complexity changes associated with noise³².

The limitations of this study include a reduced number of subjects and trials, as well as the theoretical challenge of de-

termining the optimal sliding window size for more precise noise estimation, which would mitigate the impact of transition phases between two consecutive noise powers of non-stationary noise.

Future work will focus on applying the method to new datasets with a larger number of trials and different pathophysiological conditions.

ACKNOWLEDGMENTS

The research leading to these results has received partial funding by the European Commission Horizon 2020 research and innovation programme under grant agreement No. 101017727 of the project EXPERIENCE and by the Italian Ministry of Education and Research (MIUR) in the framework of the FoReLab project (Departments of Excellence).

DATA AVAILABILITY STATEMENT

Data are publicly available. The links are reported in the method section.

The software code to compute the time-variant noise estimation is available at: https://github.com/AndScar/noise_estimation

DECLARATION OF INTEREST STATEMENT

The authors declare that they have no known competing financial interests or personal relationships that could have appeared to influence the work reported in this article.

- ¹A. Witt, J. Kurths, and A. Pikovsky, “Testing stationarity in time series,” *physical Review E* **58**, 1800 (1998).
- ²H. Kantz and T. Schreiber, *Nonlinear time series analysis*, Vol. 7 (Cambridge university press, 2004).
- ³H. D. Abarbanel, T. Carroll, L. Pecora, J. Sidorowich, and L. S. Tsimring, “Predicting physical variables in time-delay embedding,” *Physical Review E* **49**, 1840 (1994).
- ⁴A. Provenzale, L. A. Smith, R. Vio, and G. Murante, “Distinguishing between low-dimensional dynamics and randomness in measured time series,” *Physica D: nonlinear phenomena* **58**, 31–49 (1992).
- ⁵U. Rajendra Acharya, K. Paul Joseph, N. Kannathal, C. M. Lim, and J. S. Suri, “Heart rate variability: a review,” *Medical and biological engineering and computing* **44**, 1031–1051 (2006).
- ⁶P. C. Ivanov, “Long-range dependence in heartbeat dynamics,” in *Processes with long-range correlations: Theory and applications* (Springer, 2003) pp. 339–372.
- ⁷P. C. Ivanov, L. A. N. Amaral, A. L. Goldberger, S. Havlin, M. G. Rosenblum, Z. R. Struzik, and H. E. Stanley, “Multifractality in human heartbeat dynamics,” *Nature* **399**, 461–465 (1999).
- ⁸Z. He, “The control mechanisms of heart rate dynamics in a new heart rate nonlinear time series model,” *Scientific reports* **10**, 4814 (2020).
- ⁹G. Valenza, L. Citi, R. G. Garcia, J. N. Taylor, N. Toschi, and R. Barbieri, “Complexity variability assessment of nonlinear time-varying cardiovascular control,” *Scientific reports* **7**, 1–15 (2017).
- ¹⁰G. Valenza, L. Faes, L. Citi, M. Orini, and R. Barbieri, “Instantaneous transfer entropy for the study of cardiovascular and cardiorespiratory non-stationary dynamics,” *IEEE Transactions on Biomedical Engineering* **65**, 1077–1085 (2018).
- ¹¹K. Sunagawa, T. Kawada, and T. Nakahara, “Dynamic nonlinear vago-sympathetic interaction in regulating heart rate,” *Heart and vessels* **13**, 157–174 (1998).
- ¹²Y. Xue and P. Bogdan, “Constructing compact causal mathematical models for complex dynamics,” in *Proceedings of the 8th International Conference on Cyber-Physical Systems* (2017) pp. 97–107.
- ¹³G. Gupta, S. Pequito, and P. Bogdan, “Learning latent fractional dynamics with unknown unknowns,” in *2019 American Control Conference (ACC)* (IEEE, 2019) pp. 217–222.
- ¹⁴G. Gupta, C. Yin, J. V. Deshmukh, and P. Bogdan, “Non-markovian reinforcement learning using fractional dynamics,” in *2021 60th IEEE Conference on Decision and Control (CDC)* (IEEE, 2021) pp. 1542–1547.
- ¹⁵P. Bogdan, P. C. Ivanov, and S. Pequito, “Inference, causality and control in networks of dynamical systems: Data science and modeling perspectives to network physiology with implications for artificial intelligence,” (2022).
- ¹⁶E. A. Reed, G. Ramos, P. Bogdan, and S. Pequito, “The role of long-term power-law memory in controlling large-scale dynamical networks,” *Scientific Reports* **13**, 19502 (2023).
- ¹⁷M. Ghorbani and P. Bogdan, “A cyber-physical system approach to artificial pancreas design,” in *2013 International Conference on Hardware/Software Codesign and System Synthesis (CODES+ ISSS)* (IEEE, 2013) pp. 1–10.
- ¹⁸C. Yin, M. Udrescu, G. Gupta, M. Cheng, A. Lihu, L. Udrescu, P. Bogdan, D. M. Mannino, and S. Mihaicuta, “Fractional dynamics foster deep learning of copd stage prediction,” *Advanced Science* **10**, 2203485 (2023).
- ¹⁹D. Kelty-Stephen, O. D. Similton, E. Rabinowitz, and M. Allen, “Multifractal auditory stimulation promotes the effect of multifractal torso sway on spatial perception: Evidence from distance perception by blindwalking,” *Ecological Psychology* **35**, 136–182 (2023).
- ²⁰M. Malik, J. T. Bigger, A. J. Camm, R. E. Kleiger, A. Malliani, A. J. Moss, and P. J. Schwartz, “Heart rate variability: Standards of measurement, physiological interpretation, and clinical use,” *European Heart Journal* **17**, 354–381 (1996), <https://academic.oup.com/eurheartj/article-pdf/17/3/354/1312587/17-3-354.pdf>.
- ²¹A. Scarciglia, V. Catrambone, M. Bianco, C. Bonanno, N. Toschi, and G. Valenza, “Stochastic brain dynamics exhibits differential regional distribution and maturation-related changes,” *NeuroImage* **290**, 120562 (2024).
- ²²L. Glass, “Introduction to controversial topics in nonlinear science: Is the normal heart rate chaotic?” *Chaos: An Interdisciplinary Journal of Nonlinear Science* **19** (2009).
- ²³J. Hu, J. Gao, and W.-w. Tung, “Characterizing heart rate variability by scale-dependent lyapunov exponent,” *Chaos: An Interdisciplinary Journal of Nonlinear Science* **19** (2009).
- ²⁴A. Karavaev, Y. M. Ishbulatov, V. Ponomarenko, B. Bezruchko, A. Kiselev, and M. Prokhorov, “Autonomic control is a source of dynamical chaos in the cardiovascular system,” *Chaos: An Interdisciplinary Journal of Nonlinear Science* **29** (2019).
- ²⁵K. N. Aronis, R. D. Berger, H. Calkins, J. Chrispin, J. E. Marine, D. D. Spragg, S. Tao, H. Tandri, and H. Ashikaga, “Is human atrial fibrillation stochastic or deterministic?—insights from missing ordinal patterns and causal entropy-complexity plane analysis,” *Chaos: An Interdisciplinary Journal of Nonlinear Science* **28** (2018).
- ²⁶J. Zhang, A. Holden, O. Monfredi, M. R. Boyett, and H. Zhang, “Stochastic vagal modulation of cardiac pacemaking may lead to erroneous identification of cardiac “chaos”,” *Chaos: An Interdisciplinary Journal of Nonlinear Science* **19** (2009).
- ²⁷T. Buchner, M. Petelczyc, J. J. Żebrowski, A. Prejbisz, M. Kabat, A. Januszewicz, A. J. Piotrowska, and W. Szelenberger, “On the nature of heart rate variability in a breathing normal subject: a stochastic process analysis,” *Chaos: An Interdisciplinary Journal of Nonlinear Science* **19** (2009).
- ²⁸N. Wessel, M. Riedl, and J. Kurths, “Is the normal heart rate “chaotic” due to respiration?” *Chaos: An Interdisciplinary Journal of Nonlinear Science* **19** (2009).
- ²⁹V. Catrambone and G. Valenza, *Functional Brain-Heart Interplay: From Physiology to Advanced Methodology of Signal Processing and Modeling* (Springer Nature, 2021).
- ³⁰A. A. Armoundas, K. Ju, N. Iyengar, J. K. Kanters, P. J. Saul, R. J. Cohen, and K. H. Chon, “A stochastic nonlinear autoregressive algorithm reflects nonlinear dynamics of heart-rate fluctuations,” *Annals of biomedical engineering* **30**, 192–201 (2002).

- ³¹K. H. Chon, K.-P. Yip, B. Camino, D. Marsh, and N.-H. Holstein-Rathlou, "Modeling nonlinear determinism in short time series from noise driven discrete and continuous systems," *International Journal of Bifurcation and Chaos* **10**, 2745–2766 (2000).
- ³²A. Scarciglia, V. Catrambone, C. Bonanno, and G. Valenza, "Physiological noise: Definition, estimation, and characterization in complex biomedical signals," *IEEE Transactions on Biomedical Engineering* (2023).
- ³³A. Scarciglia, F. Gini, V. Catrambone, C. Bonanno, and G. Valenza, "Estimation of dynamical noise power in unknown systems," *IEEE Signal Processing Letters* **30**, 234–238 (2023).
- ³⁴T. Heldt, M. Oefinger, M. Hoshiyama, and R. Mark, "Circulatory response to passive and active changes in posture," in *Computers in Cardiology, 2003* (IEEE, 2003) pp. 263–266.
- ³⁵G. Valenza, L. Citi, J. P. Saul, and R. Barbieri, "Measures of sympathetic and parasympathetic autonomic outflow from heartbeat dynamics," *Journal of applied physiology* **125**, 19–39 (2018).
- ³⁶A. Porta, F. Gelpi, V. Bari, B. Cairo, B. De Maria, A. C. Takahashi, A. M. Catai, and R. Colombo, "Changes of the cardiac baroreflex bandwidth during postural challenges," *American Journal of Physiology-Regulatory, Integrative and Comparative Physiology* **324**, R601–R612 (2023).
- ³⁷L. B. Rowell, *Human cardiovascular control* (Oxford University Press, USA, 1993).
- ³⁸A. Porta, T. Gnechchi-Ruscione, E. Tobaldini, S. Guzzetti, R. Furlan, and N. Montano, "Progressive decrease of heart period variability entropy-based complexity during graded head-up tilt," *Journal of applied physiology* **103**, 1143–1149 (2007).
- ³⁹G. Valenza, L. Citi, E. P. Scilingo, and R. Barbieri, "Inhomogeneous point-process entropy: An instantaneous measure of complexity in discrete systems," *Physical Review E* **89**, 052803 (2014).
- ⁴⁰M. Nardelli, L. Citi, R. Barbieri, and G. Valenza, "Characterization of autonomic states by complex sympathetic and parasympathetic dynamics," *Physiological Measurement* **44**, 035004 (2023).
- ⁴¹G. Valenza, L. Citi, E. P. Scilingo, and R. Barbieri, "Point-process nonlinear models with laguerre and volterra expansions: Instantaneous assessment of heartbeat dynamics," *IEEE Transactions on Signal Processing* **61**, 2914–2926 (2013).
- ⁴²S. M. Pincus, "Approximate entropy as a measure of system complexity." *Proceedings of the National Academy of Sciences* **88**, 2297–2301 (1991).
- ⁴³A. Porta, B. De Maria, V. Bari, A. Marchi, and L. Faes, "Are nonlinear model-free conditional entropy approaches for the assessment of cardiac control complexity superior to the linear model-based one?" *IEEE Transactions on Biomedical Engineering* **64**, 1287–1296 (2016).
- ⁴⁴M. Brennan, M. Palaniswami, and P. Kamen, "Poincare plot interpretation using a physiological model of hrv based on a network of oscillators," *American Journal of Physiology-Heart and Circulatory Physiology* **283**, H1873–H1886 (2002).
- ⁴⁵A. L. Goldberger, L. A. Amaral, L. Glass, J. M. Hausdorff, P. C. Ivanov, R. G. Mark, J. E. Mietus, G. B. Moody, C.-K. Peng, and H. E. Stanley, "Physiobank, physiotoolkit, and physionet: components of a new research resource for complex physiologic signals," *circulation* **101**, e215–e220 (2000).
- ⁴⁶J. Pan and W. J. Tompkins, "A real-time qrs detection algorithm," *IEEE transactions on biomedical engineering* , 230–236 (1985).
- ⁴⁷L. Citi, E. N. Brown, and R. Barbieri, "A real-time automated point-process method for the detection and correction of erroneous and ectopic heartbeats," *IEEE transactions on biomedical engineering* **59**, 2828–2837 (2012).
- ⁴⁸G. Aston-Jones and J. D. Cohen, "An integrative theory of locus coeruleus-norepinephrine function: adaptive gain and optimal performance," *Annu. Rev. Neurosci.* **28**, 403–450 (2005).
- ⁴⁹M. Pertermann, M. Mückschel, N. Adelhöfer, T. Ziemssen, and C. Beste, "On the interrelation of 1/f neural noise and norepinephrine system activity during motor response inhibition," *Journal of neurophysiology* **121**, 1633–1643 (2019).